Cancer Research

Cancer Detection in Human Tissue Samples Using a Fiber-Tip pH Probe

Erik P. Schartner[1,2], Matthew R. Henderson[1], Malcolm Purdey[1,2,3], Deepak Dhatrak[4], Tanya M. Monro[1,2,5], P. Grantley Gill[6], and David F. Callen[7]

Abstract

Intraoperative detection of tumorous tissue is an important unresolved issue for cancer surgery. Difficulty in differentiating between tissue types commonly results in the requirement for additional surgeries to excise unremoved cancer tissue or alternatively in the removal of excess amounts of healthy tissue. Although pathologic methods exist to determine tissue type during surgery, these methods can compromise postoperative pathology, have a lag of minutes to hours before the surgeon receives the results of the tissue analysis, and are restricted to excised tissue. In this work, we report the development of an optical fiber probe that could potentially find use as an aid for margin detection during surgery. A fluorophore-doped polymer coating is deposited on the tip of an optical fiber, which can then be used to record the pH by monitoring the emission spectra from this dye. By measuring the tissue pH and comparing with the values from regular tissue, the tissue type can be determined quickly and accurately. The use of a novel lift-and-measure technique allows for these measurements to be performed without influence from the inherent autofluorescence that commonly affects fluorescence-based measurements on biological samples. The probe developed here shows strong potential for use during surgery, as the probe design can be readily adapted to a low-cost portable configuration, which could find use in the operating theater. Use of this probe in surgery either on excised or *in vivo* tissue has the potential to improve success rates for complete removal of cancers. *Cancer Res; 76(23); 6795–801. ©2016 AACR.*

Downloaded from http://aacrjournals.org/cancerres/article-pdf/76/23/6795/2743863/6795.pdf by guest on 10 November 2024

Introduction

Incomplete removal of malignant tumors continues to be a significant issue in cancer surgery. It increases the risk of local recurrence and impaired survival and results in the need for additional surgery with associated attendant costs and morbidity (1–3). The excision of further benign tissue leads to poor cosmesis and impaired function, which assumes particular significance in some sites, such as breast or head and neck cancer (1).

In the case of breast cancer, reexcision rates in excess of 20% have been widely reported, and this may lead to local recurrence (4–6). Standard pathology techniques, such as the use of intraoperative cytology, selective margin reexcision based on specimen imaging, and/or frozen section, are time consuming, can potentially compromise postoperative pathologic analysis, and show difficulty in accurate detection of small tumors (7–9). A recent trial reported higher rate of complete excision following systematic reexcision of the whole cavity at the time of partial mastectomy, compared with standard practice (5). Optical-based imaging technologies have been shown to distinguish malignant from benign breast tissue in exploratory studies. These include methodology based on Raman spectroscopy (10, 11), scanning *in situ* spectroscopy and mapping of whole specimens (12), combined diffuse reflectance spectroscopy and intrinsic autofluorescence (10, 13), or multimodal optical imaging (14). These studies have been exploratory and have examined and mapped tissue distribution in whole excised specimens *ex vivo*. Potential limitations to their clinical use include the portability of equipment, tissue heterogeneity leading to scattering of light and autofluorescence, and the time required to complete assessments.

The further development of rapid real-time techniques to detect small volumes of cancer at the margins of surgical specimens continues to be a priority in the treatment of cancer. Although breast cancer has been the principal focus of such investigations, the technology is also potentially important in other sites (15).

It has been shown in the literature that the extracellular pH in the vicinity of cancer is lowered, when compared with that of normal tissue in the same patient (16–19). Although various methods exist to record tissue pH, to date, it has been found to be difficult to accurately measure the pH of small areas of tissue as would be required for the detection of cancer margins due primarily to the large size of conventional electrochemical surface pH probes, which typically have a tip diameter in the order of 10 mm.

Optical fiber–based sensors have found extensive use in the areas of chemical (20–24), biological sensing (25–27), physical sensing for temperature (28–30), or structural health monitoring

[1]Institute for Photonics and Advanced Sensing, School of Physical Sciences, The University of Adelaide, Adelaide, Australia. [2]ARC Centre for Nanoscale BioPhotonics, The University of Adelaide, Adelaide, Australia. [3]Heart Health Theme, South Australian Health and Medical Research Institute, Adelaide, Australia. [4]Department of Anatomical Pathology, Adelaide, Australia. [5]University of South Australia, Adelaide, Australia. [6]Department of Surgery, University of Adelaide & Breast, Endocrine & Surgical Oncology Unit, Royal Adelaide Hospital, Adelaide, Australia. [7]Centre for Personalised Cancer Medicine, School of Medicine, University of Adelaide, Adelaide, Australia

E.P. Schartner and M.R. Henderson are co-first authors of this article and contributed equally to this article.

Corresponding Author: Erik P. Schartner, University of Adelaide, North Tce, Adelaide, South Australia 5005, Australia. Phone: 6104-0352-6202; Fax: 6108-8313-5316; E-mail: erik.schartner@adelaide.edu.au

doi: 10.1158/0008-5472.CAN-16-1285

©2016 American Association for Cancer Research.

(31, 32). Typically, they are deployed in situations where measurements along the length of the fiber (distributed measurements) are required (33); however, they also have strong potential for use in applications in difficult to reach locations. Fiber measurements can be performed at a position remote from the source and detection equipment. By creating a functional coating either along the length of the fiber, or on the end-face, the sensing region can be localized to the desired location depending on the application.

Here, we report the first tissue pH measurements performed with an optical fiber-tip pH probe on excised cancer samples. The optical fiber probe measures pH rapidly, in less than one minute, is simple to use, and does not leave a residue or stain that would affect later pathology testing. The probe consists of the pH-sensitive fluorophore 5,6-carboxynapthofluorescein (CNF; ref. 23), which changes color with a change in the environmental pH. This fluorophore is embedded in an acrylamide polymer on the optical fiber tip, which is read out remotely via a laser at the other end of the fiber. Preliminary testing showed that this indicator displayed a good balance of an appropriate pH response range, broad optical spectra that could potentially be interrogated in the future with bulk optics, and good stability for repeat measurements over time. The fiber probe is flexible and robust and has a small measurement area corresponding to the size of the 200-μm diameter optical fiber tip.

Measurements using organic fluorophores are commonly performed by monitoring the emission intensity of a single fluorescence band (wavelength), which is susceptible to errors arising from variations in the excitation light power or photobleaching of the dye. With CNF, the pH value is inferred by monitoring the ratio of two emission bands of the fluorophore. Ratiometric methods alleviate potential issues from photobleaching or coupling, allowing for measurements to be performed over a long period without the introduction of systematic errors.

A pervasive issue with optical-based measurements of chemical or biological parameters is the presence of background autofluorescence from the tissue itself, which is generated when the excitation light is incident on the tissue sample (34). Although this can be reduced through the use of longer wavelength excitation sources, or prebleaching of the tissue, it remains a limitation in the majority of approaches to determine tissue measurements. This autofluorescence signal is difficult to remove through signal postprocessing, as it can vary significantly across a single sample (34). The novel architecture presented here can be utilized in a manner that avoids tissue autofluorescence impacting on the pH measurement. Here, the fiber-tip probe is placed in contact with the tissue surface and allowed to equilibrate and is then lifted from the surface before the fluorophore is measured. This new "lift-and-measure" technique removes the interaction between the excitation source and the sample tissue. The fluorophore chemical structure is altered under different environmental pH conditions, which determines the varying emission properties. We propose that the sampling measurement induced structural change in the fluorophore is retained after lifting from the surface, and so, the pH can be measured in the absence of autofluorescence. Calibration curve pH measurements were performed in a series of phosphate buffers, and these confirmed that a comparable response was seen between measurements with the probe dipped into the buffer and after lifting out from the buffer in air.

Using these techniques, surgically excised human breast cancer and melanoma tissue samples were measured with the optical fiber pH probe at numerous locations over the sample surface, with the tissue type of each location confirmed later by histopathology.

Materials and Methods

Materials

Acrylamide (99%), *N,N′*-methylenebis(acrylamide) (99%), 3-(trimethoxysilyl)propyl methacrylate (98%), triethylamine (99%), and monobasic and dibasic potassium hydrogen phosphate were obtained from Sigma-Aldrich Chemical Co. CNF was obtained from Santa Cruz Biotechnology. Potassium phosphate buffers were made up from appropriate ratios of monobasic and dibasic potassium hydrogen phosphate to an ionic strength of 0.1 mmol/L, covering a pH range from 6.0 to 8.8.

The polymer solution consisted of (by weight) 27% acrylamide, 3% bis-acrylamide, and 70% pH 6.5 potassium phosphate buffer, with 0.4 mg/mL CNF and 40 μL/mL triethylamine. The solution was ultrasonicated until all solid components were fully dissolved and used immediately.

Fiber probe

The optical setup was configured as shown in Fig. 1. Acrylamide was attached to the fiber tip by photopolymerization using a 405-nm laser for two seconds at a coupled power of 13 mW. The CNF fluorophore was excited with a blue 473-nm laser for the pH measurements. The two lasers were aligned to be collinear into the microscope objective, such that no realignment was required between the coating step and subsequent measurements. Silica multi-mode fiber was used for all coating trials (Thorlabs UG200UEA or Ocean Optics 200 μm UV/VIS).

The fiber was cleaved to expose a fresh surface for polymer attachment. The fiber tip was dipped into a 2% solution of 3-(trimethoxysilyl)propyl methacrylate in pH 3.5 HCl for one hour, after which the fiber was removed and dried with nitrogen. A 405-nm laser source (CrystaLaser 25 mW) was coupled into the input end of the optical fiber, and the power optimized with a calibrated photodiode. Fiber tips were then dipped into the acrylamide polymer solution described above and illuminated

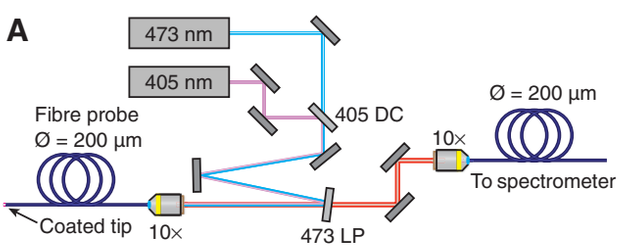

Figure 1.
Experimental details for measurements. **A,** Schematic for coating and pH measurement trials. **B,** Scanning electron microscope image showing an example of the polymer coatings obtained.

Downloaded from http://aacrjournals.org/cancerres/article-pdf/76/23/6795/2743863/6795.pdf by guest on 10 November 2024

with the 405-nm source for two seconds with a coupled laser power of 15 ± 0.2 mW to photopolymerize the acrylamide polymer onto the fiber tip.

pH measurement

A schematic of the optical setup is shown in Fig. 1. A 473-nm laser (Toptica iBeam Smart) was used to excite the CNF fluorophore. The resulting emission of the CNF consists of two peaks, at approximately 565 and 705 nm, with an intensity ratio dependent on the pH of the environment around the fluorophore.

To excite the CNF fluorophore, the 473-nm laser was coupled into the distal end of the probe fiber. The coupled laser light then excites the fluorophore-doped probe tip, and a portion of this fluorescent light is then captured into a back-propagating mode in the fiber. The fluorescent signal then passes through a 473-nm long-pass filter (Semrock EdgeBasic) to remove excess excitation light, before being coupled into a spectrometer (Horiba iHR320) via a 200-μm optical fiber patch cable.

As the surface pH of tissue biopsies deteriorated slowly when exposed to the atmosphere, before measuring with the probe, fresh surfaces were exposed by excision.

Spectral analysis and lift-and-measure measurement technique

The ratio of the two CNF fluorophore emission peaks was used to measure the pH response of the probe. Spectra were postprocessed by integrating the signal under two peaks, from 500 to 635 nm and from 635 to 900 nm, and dividing the area of the first peak by the area of the second peak giving the fluorescence ratio for that particular probe location.

Samples were first measured with the probe tip in contact with the sample. The probe was then lifted from the surface, and the measurement repeated. Removal of the probe tip from the sample eliminates autofluorescence from the tissue sample, such that the only contribution to the observed signal is from the fiber sensor itself.

Probe verification

The pH response of the optical fiber probe was verified by dipping into a series of 0.1 mmol/L potassium phosphate buffer solutions. Measurements were performed both in the solution and in air after removing from the buffer, to simulate the lift-and-measure technique described above and as used for the human tissue samples.

Autofluorescence measurements

Sheep tissue samples were spiked with 1 mol/L hydrochloric acid (Sigma-Aldrich) or 1 mol/L sodium hydroxide (Sigma-Aldrich) to obtain acidic or basic samples, respectively. Measurements were performed using the lift-and-measure technique described above, in an identical fashion to that used for the human tissue samples.

Tissue samples

The project was approved by the Royal Adelaide Hospital Research Ethics Committee, and patients gave individual informed consent for their participation.

Research specimens obtained at surgery were placed on ice and transported to the pathology laboratory, where they were inked and sliced for normal diagnostic processing. Four mastectomy specimens, one axillary clearance for recurrent breast cancer, and three cases of metastatic melanoma were included (Table 1). Fresh tissue not required for diagnostic evaluation was utilized for the pH evaluation experiments within one hour of excision at surgery.

Pathology verification

The location of each pH measurement using the optical fiber probe was photographically recorded to enable correlation with the presence of nonmalignant or cancer tissue as determined by subsequent histopathology.

Following the pH measurements, the tissue was fixed in 10% buffered formalin for 24 hours and photographed. The presence of cancer or normal tissue at the measurement sites was then histologically assessed in hematoxylin and eosin (H&E)–stained paraffin-embedded sections. The occurrence of either cancer or normal tissue at each measurement site was determined by using both the macroscopic photographs and the H&E-stained sections for accuracy. The H&E sections were also used for tumor typing and determination of nonmalignant tissue as fat or fibrosis. Correlation was then made with the site of probe and the type of underlying tissue from which the pH reading was taken. For the majority of the cases, there was a single localized tumor, but several cases had multifocal tumors in the specimen (Table 1).

Results

Effect of tissue autofluorescence

A background tissue autofluorescence signal is generated when the probe excitation light is incident on the tissue sample. The autofluorescence spectrum can vary significantly across the sample and so is difficult to remove with data postprocessing techniques, such as subtraction. An example of tissue autofluorescence is shown in Fig. 2, where spectra have been recorded with the probe both touching and lifted from the tissue surface, for sheep

Table 1. Summary of measurements

Sample	Specimen	Tumor type	Number of measurements	Tumor mean and SD	Normal mean and SD
1	Left inguinal lymph node dissection	Metastatic melanoma	12	5.3 ± 1.3	1.0 ± 0.1
2	Left axillary clearance	Metastatic melanoma in multiple lymph nodes	11	3.4 ± 1.0	1.0 ± 0.07
3	Skin excision, right groin	Subcutaneous deposit of metastatic melanoma	15	1.7 ± 0.4	1.0 ± 0.5
4	Left mastectomy	Grade 2 infiltrating ductal carcinoma	12	1.31 ± 0.31	1.0 ± 0.2
5	Left mastectomy	Grade 2 infiltrating ductal carcinoma	11	2.7 ± 1.5	1.0 ± 0.8
6	Right mastectomy	Invasive metaplastic carcinoma (spindle cell carcinoma with anaplasia)	20	3.3 ± 0.8	1.0 ± 0.4
7	Left mastectomy	Grade 3 infiltrating ductal carcinoma	11	6.9 ± 2.6	1.0 ± 0.04
8	Left axillary clearance	Multiple tumor deposits of infiltrating ductal carcinoma ranging 4 to 20 mm	12	1.9 ± 0.3	1.0 ± 0.1

Downloaded from http://aacrjournals.org/cancerres/article-pdf/76/23/6795/2743863/6795.pdf by guest on 10 November 2024

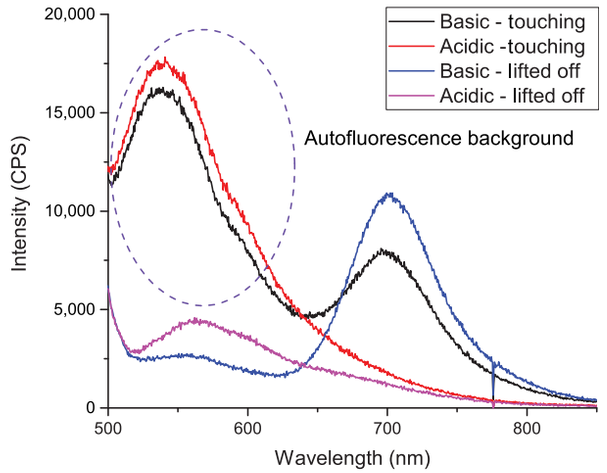

Figure 2.
Spectra of fiber pH probe measuring the surface of tissue spiked with an acidic or basic solution. Measurements were performed both touching the tissue surface and in air using the lift-and-measure technique.

tissue samples spiked with hydrochloric acid (acidic) or sodium hydroxide (basic) solutions.

As shown in Fig. 2, the autofluorescence background can form a significant fraction of the total signal strength and can form a significant contribution to the apparent measured ratio. The tissue samples were spiked with acidic and basic solutions to show that the autofluorescence background affects measurements in both high and low pH environments

Probe response to pH and verification of lift-and-measure technique

To reduce the impact of autofluorescence on the pH measurements a novel "lift-and-measure" technique was devised. The probe response to pH was first recorded with a series of PBS buffer solutions, measuring the response both before and after removal from the solution (Fig. 3).

From these results, it can be seen that the probe has a similar response to pH both in solution and after removal, with a small shift in the pH response curve between the two, and so it can be concluded that the lift-and-measure pH measurement is a valid reading of the surface tissue pH. Upon removal of the fiber from the solution, changes in the fluorescence spectra were observed for 1 to 5 seconds, which is interpreted as the evaporation of the solvent from the tip of the fiber. After this rapid change, the signal was observed to be stable for a period of at least 10 minutes. Preliminary experiments demonstrated that the pH shift of this fluorophore was extremely well suited to differentiation between healthy and tumorous tissue, with large shifts observed in the fluorescence ratio between the two tissue types.

Figure 3A shows the fluorescence response of the CNF with varied pH. As the buffer pH increases, the first peak decreases in intensity, while the second peak increases. Integration of the two fluorescence bands to obtain the fluorescence ratio gives the results shown in Fig. 3B. This ratiometric behavior allows for the pH to be interpreted with little dependence on the excitation power or fluorophore density. If the excitation intensity is increased, the two bands will increase proportionally, removing the intensity dependence, which typically restricts the precision of intensity-based fluorophore measurements. This property also minimizes variations in pH signal response between probes, simplifying fabrication requirements.

The structure of CNF both before and after reaction with hydrogen ions is shown in Fig. 4. As the probe equilibrates with the pH of the solution, each CNF molecule will be in either the protonated acid form or in the deprotonated form that favors formation of the lactone. We postulate that because each CNF molecule is locked in protonated or deprotonated form, the fluorescence emission profile of the probe will reflect the equilibrium achieved in solution. The subsequent result of this is that the probe retains a "memory" of the pH of the solution into which it was last immersed. This particular property of the fluorophore

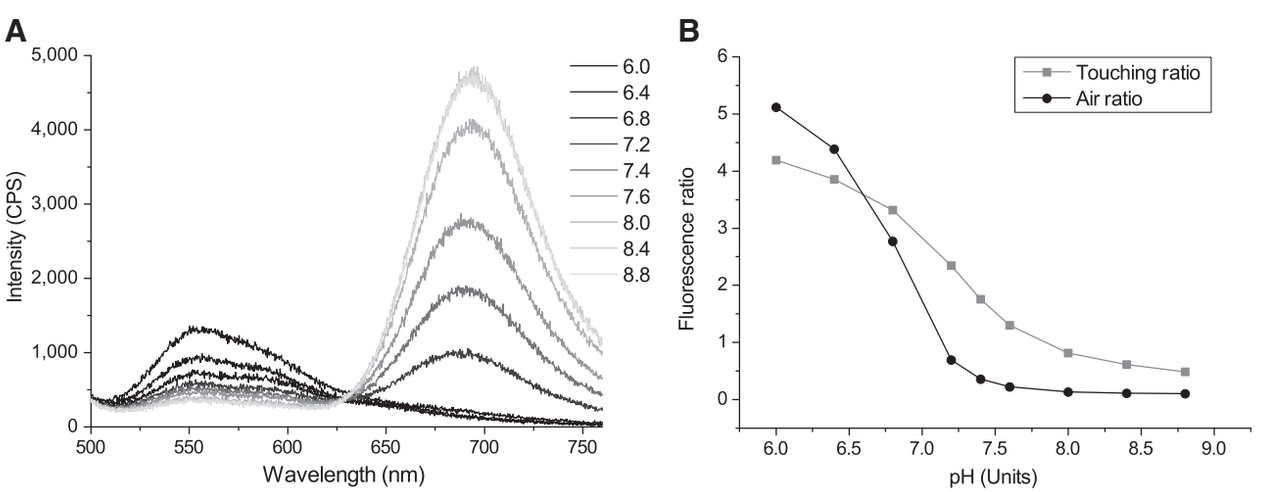

Figure 3.
Characterization of the polymer functionalized probe. **A,** Emission spectra of the CNF fluorophore at different environmental pH values showing the ratiometric response. Spectra taken in air after 20-second immersion in buffer. **B,** Calibration curve for the fiber pH probe both dipped into a buffer (touching, gray squares) and in air after dipping (air, black circles).

Downloaded from http://aacrjournals.org/cancerres/article-pdf/76/23/6795/2743863/6795.pdf by guest on 10 November 2024

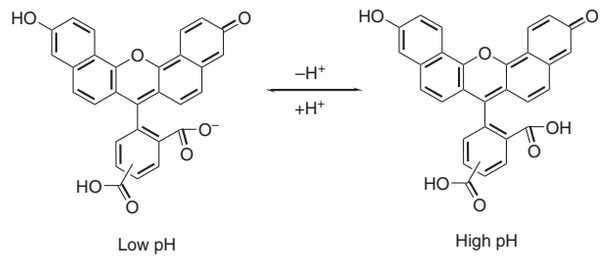

Figure 4.
Chemical structure of CNF, illustrating the structural change that occurs due to pH.

allows for the use of the lift-and-measure technique, with measurements to be performed after the removal of the probe from the surface of the tissue sample to reduce the observed tissue autofluorescence.

Tissue measurements

Tissue surface measurements were obtained from four melanoma and four breast cancer samples. Figure 5A shows the individual measurement results, with tissue type determined after each experiment by pathology tests. Data were normalized to the mean value of the normal tissue results to simplify comparison between samples, the results of which are shown in Fig. 5A. The mean and SD values for the individual samples are shown in Table 1, along with descriptions of the specimen and tumor type for each of the measured samples. The ROC curve for the normalized data is shown in Fig. 5B.

An example of a measured sample is shown in Fig. 6 below. This photograph, taken before optical measurements were performed, has the probe sampling locations marked for sample 2 (metastatic melanoma in multiple lymph nodes). The tissue type in each of these locations was determined using pathologic analysis methods described earlier.

From the results shown in Fig. 5A, it can be seen that typically, the tumor samples are significantly more acidic than normal tissue samples. Applying the Mann–Whitney *U* test on the dataset showed significant differences between healthy and tumorous tissue, with $P < 0.001$. Utilizing the ROC curve in Fig. 5B, a threshold for these preliminary values was defined, with a pH ratio of 1.35 showing a sensitivity of 88% and a selectivity of 90%.

As can be seen from the data in Table 1, some variation in values is observed between samples for the tumor tissue samples, with the majority of samples, however, still showing a statistically significant difference in tissue pH between the tumor and normal tissue samples.

Necrotic tumor and fibrosis tissue types were also measured during trials, with results suggesting that the probe is also able to discriminate effectively between these tissue types as well. Necrotic tumor samples were observed to display a similar pH to regular cancer samples, whereas fibrosis samples showed a similar pH to normal tissue.

Discussion

These results show that cancerous tissue can be effectively differentiated from normal tissue in fresh human tissue biopsies by measurement of the tissue pH. The use of an optical probe allows for measurements to be performed rapidly with high spatial resolution. Currently, our results show that measurements can be performed using an optical probe with a diameter of 200 μm, equivalent to an area in the order of five to ten cells wide, with the potential to reduce this to the measurement of single cells by reducing the size of the fiber probe

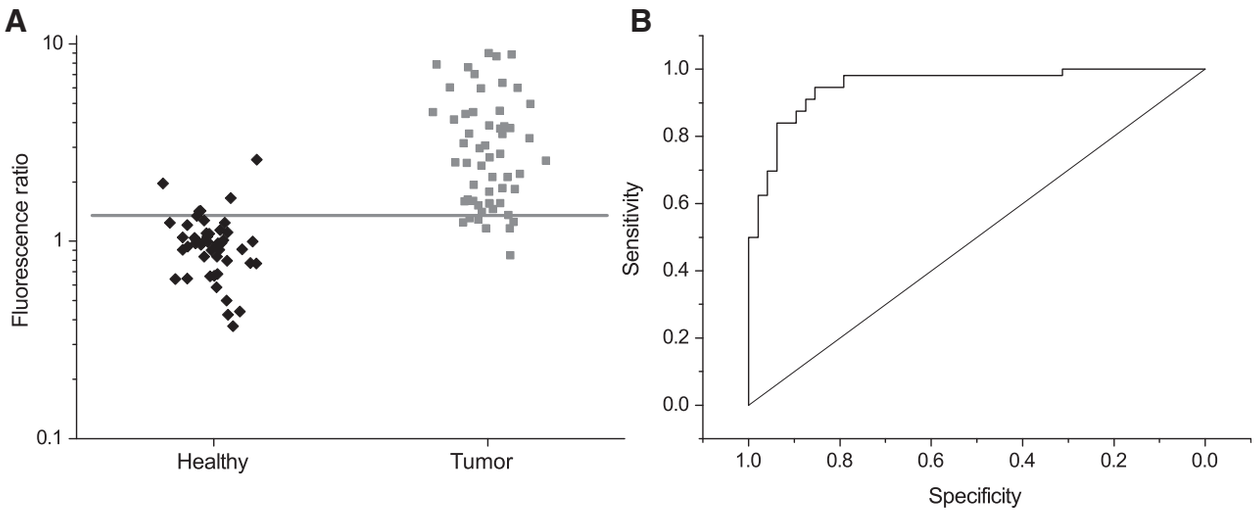

Figure 5.
Results obtained from use of the optical fiber pH probe on excised human tissue samples. **A,** Scatter plot showing the measured fluorescence ratio using the optical fiber-tip pH probe, obtained from normal (fat and breast tissue) and tumor surface tissue measurements across eight tissue samples. Probe measurement locations were subsequently pathology tested to confirm tissue type. For each sample, the data were normalized to the mean value of the corresponding normal tissue dataset, with the mean and SD for each individual sample shown in Table 1. Tumor (gray) and normal (black) measurement datasets are shown, with the experimentally derived threshold value used to determine the accuracy and specificity of the optical measurement technique marked in gray. **B,** ROC curve for data shown in A.

Downloaded from http://aacrjournals.org/cancerres/article-pdf/76/23/6795/2743863/6795.pdf by guest on 10 November 2024

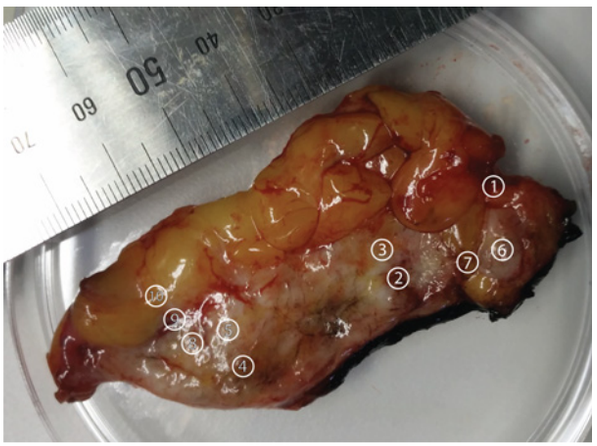

Figure 6.
Example photograph of sample 2 (metastatic melanoma in multiple lymph nodes), with probe sampling locations marked on the image.

by tapering the fiber tip (25). The use of the lift-and-measure technique allows measurements to be performed without the influence of the tissue autofluorescence that typically restricts the performance of optical sensors. Minimal effects from photobleaching were observed, with the sensor showing high levels of stability even with repeat scans during tissue measurements.

The performance of the pH probe in this preliminary study was comparable or exceeded that described by a commercially available product, the MarginProbe (88% sensitivity at 1.35 threshold marked in Fig. 5A, versus 84%–68%) by Pappo and colleagues (35, 36). The variations observed a subset of the tissue samples may have been due to probe function or, alternatively, failure to accurately collocate the tissue measurement and the final pathology samples. Measures to address this latter possibility have been included in current studies. Heterogeneity of tissue elements can vary widely within tumors and normal breast tissue. This was shown to contribute to a variation in sensitivity in the detailed initial evaluation of the MarginProbe by Pappo and colleagues (35). Similar criticisms have been made with respect to the range of other optical methods (37). A similar consideration could have contributed to the variation we observed with low values for two tumors.

Additional improvements to the optical probe, such as the use of multi-core imaging fiber, could also result in an increase in sample throughput, by measuring the tissue pH over a larger area with improved spatial resolution compared with the multi-mode fiber that was utilized here, which gives a single discrete pH measurement at each sampling location.

This is an important step toward the development of a real-time sensor that can be used *in vivo* at the time of surgery to determine the presence of cancer at surgical margins. The rapid response of the optical probe gives an indication of the tissue type in real time. Measurement time could potentially be controlled by varying the thickness of the polymer layer, as testing showed a thinner layer gives faster response, however, at the cost of reduced signal intensity. The use of such a fiber sensor to give an immediate indication of tissue type has the potential to reduce the need for repeat surgery by increasing the success rate of complete cancer removal. It offers the potential for greater precision and smaller excision volumes during surgery compared with a complete cavity shave (5) and a small footprint compared with other techniques. The low level of complexity involved in determining tissue type using the probe also gives rise to the potential for the use of this probe in a portable configuration. Given its construction is based on optical fibers, it also has the potential for wider use in other sites and more deeply situated tumors as allowed by endoscopic or image-guided devices.

Disclosure of Potential Conflicts of Interest

T.M. Monro is the deputy vice chancellor at University of South Australia. No potential conflicts of interest were disclosed by the other authors.

Authors' Contributions

Conception and design: M.R. Henderson, D. Dhatrak, T.M. Monro, P.G. Gill, D.F. Callen
Development of methodology: E.P. Schartner, M.R. Henderson, D. Dhatrak, T.M. Monro
Acquisition of data (provided animals, acquired and managed patients, provided facilities, etc.): E.P. Schartner, M.R. Henderson, D. Dhatrak, P.G. Gill
Analysis and interpretation of data (e.g., statistical analysis, biostatistics, computational analysis): E.P. Schartner, M.R. Henderson, M. Purdey, D. Dhatrak, P.G. Gill, D.F. Callen
Writing, review, and/or revision of the manuscript: E.P. Schartner, M.R. Henderson, M. Purdey, D. Dhatrak, T.M. Monro, P.G. Gill, D.F. Callen
Administrative, technical, or material support (i.e., reporting or organizing data, constructing databases): E.P. Schartner, M.R. Henderson, D. Dhatrak, P.G. Gill
Study supervision: T.M. Monro, P.G. Gill

Acknowledgments

The authors would like to thank Prof. Mark Hutchinson for assistance with statistical analysis, Dr. Georgios Tsiminis for useful discussions, and Sebastian Ng and Catherine Lang for assistance with some of the experiments.

Grant Support

The authors acknowledge funding support from the National Breast Cancer Foundation Australia, an Australian Research Council linkage projectLP110200736, and an ARC Georgina Sweet Laureate Fellowship.

Received May 18, 2016; revised August 24, 2016; accepted September 13, 2016; published OnlineFirst November 30, 2016.

References

1. Cabioglu N, Hunt KK, Sahin AA, Kuerer HM, Babiera GV, Singletary SE, et al. Role for intraoperative margin assessment in patients undergoing breast-conserving surgery. Ann Surg Oncol 2007;14:1458–71.
2. Rouzier R, Extra J-M, Carton M, Falcou M-C, Vincent-Salomon A, Fourquet A, et al. Primary chemotherapy for operable breast cancer: incidence and prognostic significance of ipsilateral breast tumor recurrence after breast-conserving surgery. J Clin Oncol 2001;19:3828–35.
3. Elkhuizen PH, van de Vijver MJ, Hermans J, Zonderland HM, van de Velde CJ, Leer J-WH. Local recurrence after breast-conserving therapy for invasive breast cancer: high incidence in young patients and association with poor survival. Int J Radiat Oncol Biol Phys 1998;40:859–67.
4. Jeevan R, Cromwell D, Trivella M, Lawrence G, Kearins O, Pereira J, et al. Reoperation rates after breast conserving surgery for breast cancer among women in England: retrospective study of hospital episode statistics. BMJ 2012;345:e4505.
5. Chagpar AB, Killelea BK, Tsangaris TN, Butler M, Stavris K, Li F, et al. A randomized, controlled trial of cavity shave margins in breast cancer. N Engl J Med 2015;373:503–10.

Downloaded from http://aacrjournals.org/cancerres/article-pdf/76/23/6795/2743863/6795.pdf by guest on 10 November 2024

6. McCahill LE, Single RM, Bowles EJA, Feigelson HS, James TA, Barney T, et al. Variability in reexcision following breast conservation surgery. JAMA 2012;307:467–75.
7. Pleijhuis RG, Graafland M, de Vries J, Bart J, de Jong JS, van Dam GM. Obtaining adequate surgical margins in breast-conserving therapy for patients with early-stage breast cancer: current modalities and future directions. Ann Surg Oncol 2009;16:2717–30.
8. Singletary SE. Surgical margins in patients with early-stage breast cancer treated with breast conservation therapy. Am J Surg 2002;184:383–93.
9. Unzeitig A, Kobbermann A, Xie X-J, Yan J, Euhus D, Peng Y, et al. Influence of surgical technique on mastectomy and reexcision rates in breast-conserving therapy for cancer. Int J Surg Oncol 2012;2012.
10. Keller MD, Vargis E, de Matos Granja N, Wilson RH, Mycek M-A, Kelley MC, et al. Development of a spatially offset Raman spectroscopy probe for breast tumor surgical margin evaluation. J Biomed Opt 2011;16:077006.
11. Haka AS, Volynskaya Z, Gardecki JA, Nazemi J, Lyons J, Hicks D, et al. *In vivo* margin assessment during partial mastectomy breast surgery using Raman spectroscopy. Cancer Res 2006;66:3317–22.
12. Krishnaswamy V, Laughney AM, Wells WA, Paulsen KD, Pogue BW. Scanning *in situ* spectroscopy platform for imaging surgical breast tissue specimens. Optics Exp 2013;21:2185–94.
13. Lue N, Kang JW, Yu C-C, Barman I, Dingari NC, Feld MS, et al. Portable optical fiber probe-based spectroscopic scanner for rapid cancer diagnosis: a new tool for intraoperative margin assessment. PLoS One 2012;7:e30887.
14. Patel R, Khan A, Wirth D, Kamionek M, Kandil D, Quinlan R, et al. Multimodal optical imaging for detecting breast cancer. J Biomed Opt 2012;17:066008.
15. Poh CF, Zhang L, Anderson DW, Durham JS, Williams PM, Priddy RW, et al. Fluorescence visualization detection of field alterations in tumor margins of oral cancer patients. Clin Cancer Res 2006;12:6716–22.
16. Gerweck LE. Tumor pH: implications for treatment and novel drug design. Semin Radiat Oncol 1998;8:176–82.
17. Gerweck LE, Seetharaman K. Cellular pH gradient in tumor versus normal tissue: potential exploitation for the treatment of cancer. Cancer Res 1996;56:1194–98.
18. Stubbs M, McSheehy PM, Griffiths JR, Bashford CL. Causes and consequences of tumour acidity and implications for treatment. Mol Med Today 2000;6:15–19.
19. Švastová E, Hulíková A, Rafajová M, Zat'ovičová M, Gibadulinová A, Casini A, et al. Hypoxia activates the capacity of tumor-associated carbonic anhydrase IX to acidify extracellular pH. FEBS Lett 2004;577:439–45.
20. Wolfbeis OS. Fiber-optic chemical sensors and biosensors. Anal Chem 2008;80:4269–83.
21. Warren-Smith SC, Heng S, Ebendorff-Heidepriem H, Abell AD, Monro TM. Fluorescence-based aluminum ion sensing using a surface-functionalized microstructured optical fiber. Langmuir 2011;27:5680–85.
22. Peterson JI, Goldstein SR, Fitzgerald RV, Buckhold DK. Fiber optic pH probe for physiological use. Anal Chem 1980;52:864–69.
23. Song A, Parus S, Kopelman R. High-performance fiber-optic pH microsensors for practical physiological measurements using a dual-emission sensitive dye. Anal Chem 1997;69:863–67.
24. Schartner EP, Tsiminis G, François A, Kostecki R, Warren–Smith SC, Nguyen LV, et al. Taming the light in microstructured optical fibers for sensing. Int J Appl Glass Sci 2015;6:229–39.
25. Tan W, Shi Z-Y, Smith S, Birnbaum D, Kopelman R. Submicrometer intracellular chemical optical fiber sensors. Science 1992;258:778–81.
26. Shortreed M, Kopelman R, Kuhn M, Hoyland B. Fluorescent fiber-optic calcium sensor for physiological measurements. Anal Chem 1996;68:1414–18.
27. Warren-Smith SC, Nie G, Schartner EP, Salamonsen LA, Monro TM. Enzyme activity assays within microstructured optical fibers enabled by automated alignment. Biomed Optics Expr 2012;3:3304–13.
28. Hocker G. Fiber-optic sensing of pressure and temperature. Appl Opt 1979;18:1445–8.
29. Kurashima T, Horiguchi T, Tateda M. Distributed-temperature sensing using stimulated Brillouin scattering in optical silica fibers. Opt Lett 1990;15:1038–40.
30. Schartner EP, Monro TM. Fibre tip sensors for localised temperature sensing based on rare earth-doped glass coatings. Sensors 2014;14:21693–701.
31. Tennyson R, Mufti A, Rizkalla S, Tadros G, Benmokrane B. Structural health monitoring of innovative bridges in Canada with fiber optic sensors. Smart Mat Struct 2001;10:560.
32. Majumder M, Gangopadhyay TK, Chakraborty AK, Dasgupta K, Bhattacharya DK. Fibre Bragg gratings in structural health monitoring—Present status and applications. Sens Actuators A 2008;147:150–64.
33. Bao X, Webb DJ, Jackson DA. 32-km distributed temperature sensor based on Brillouin loss in an optical fiber. Opt Lett 1993;18:1561–63.
34. Neumann M, Gabel D. Simple method for reduction of autofluorescence in fluorescence microscopy. J Histochem Cytochem 2002;50:437–39.
35. Pappo I, Spector R, Schindel A, Morgenstern S, Sandbank J, Leider LT, et al. Diagnostic performance of a novel device for real-time margin assessment in lumpectomy specimens. J Surg Res 2010;160:277–81.
36. Allweis TM, Kaufman Z, Lelcuk S, Pappo I, Karni T, Schneebaum S, et al. A prospective, randomized, controlled, multicenter study of a real-time, intraoperative probe for positive margin detection in breast-conserving surgery. Am J Surg 2008;196:483–89.
37. Thill M, Röder K, Diedrich K, Dittmer C. Intraoperative assessment of surgical margins during breast conserving surgery of ductal carcinoma in situ by use of radiofrequency spectroscopy. Breast 2011;20:579–80.

Downloaded from http://aacrjournals.org/cancerres/article-pdf/76/23/6795/2743863/6795.pdf by guest on 10 November 2024